Journal of Applied Polymer Science

Patterning of conducting layers on breathable substrates using laser engraving for gas sensors

Bartlomiej Kolodziejczyk, Orawan Winther-Jensen, Brooke A. Pereira, Santhosh S. Nair, Bjorn Winther-Jensen

Department of Materials Engineering, Monash University, Clayton, Victoria 3800, Australia

Correspondence to: B. Kolodziejczyk (E-mail: bartlomiej.kolodziejczyk@monash.edu)

ABSTRACT: Most of the techniques used for micro and nano-patterning currently are of high quality and reproducibility, but they require expensive equipment and involve many time-consuming steps to achieve the desired results. We herein report a patterning method of conducting layers on breathable substrates using a fast, simple, and mask-less laser engraving technique. A resolution in the range of 30 μm has been successfully achieved in this report. The method is fast and the pattern can be easily changed or redesigned within a few minutes. The patterning time for a 25 cm^2 sample is approximately 3 minutes. In comparison, patterning a sample of the same size using photolithography requires up to 4 hours. In this manuscript, we describe the laser patterning process, how to improve the patterning resolution, the calibration steps involved as well as an application for organic electrochemical transistors as gas sensors for detecting oxygen or sulphur dioxide. © 2015 Wiley Periodicals, Inc. J. Appl. Polym. Sci. **2015**, *132*, 42359.

KEYWORDS: conducting polymers; membranes; sensors and actuators

Received 25 November 2014; accepted 11 April 2015

DOI: 10.1002/app.42359

INTRODUCTION

Micro-patterning plays an important role in nowadays' electronics. The manufacturing process has to be fast, cheap, simple, efficient and scalable. Organic electrochemical transistor (OECT) is one of the electronic components that uses micro-patterning. The most common process used to pattern OECT is photolithography (e.g., shadow mask patterning procedure) which requires expensive machines, is time consuming and involves many complicated processing steps.[1–3] The first expense in mask patterning is that the mask has to be designed and manufactured before patterning can even start. Developing fast and robust routes to produce patterns of electrically conducting materials on various isolating substrates has been an ongoing area of research for decades and is providing the "baseline" for all produced electrical and electronic circuits. The use of laser equipment to cut and engrave materials is well established and used extensively throughout a wide range of industries.[4–12] The resolution of the resulting pattern is dependent on the quality of the laser engraver and is adjustable by following the parameters from the calibration. The particular "delicate" substrate used in the current manuscript is a porous breathable membrane based on polytetrafluoroethylene (PTFE) which was successfully used in previous studies to implement a three phase interface concept to breathe gases in as well as out of the electrochemical cells.[13–16] The electrochemical reactions occur at the point of contact between the gas, the poly (3,4-ethylenedioxythiophene) (PEDOT) electrode and the electrolyte. In the reports mentioned above,[13–16] the electrochemical detection occurred using a conventional three electrode electrochemical set-up. For the present study, the porous PTFE substrate is used to breathe in the gases for the OECT gas sensor set-up.

Conducting polymers (CPs) have proved to be great candidates for OECTs,[17–19] where traditional silicon or copper circuits are replaced with its organic counterparts. CPs bring many advantages, the main being they are easy and cheap to manufacture and their properties can be tunable. Also, they are flexible and hence can be used in flexible or wearable devices[20–22] and have a better interface with biological materials and living cells.[18,23,24] The CP used in this report was PEDOT, an intrinsically conductive polymer, favored for electrochemical applications due to its relative stability and high conductivity.[13,25–27] There are several approaches to the manufacture of CP layers[28–31] and it is appreciated that the ones used in this report are not the only possibilities.

The laser patterning approach was further investigated to pattern other conducting layers such as metals and graphene which have been deposited on the flexible/porous substrates. For

Additional Supporting Information may be found in the online version of this article.

© 2015 Wiley Periodicals, Inc.

cutting or engraving materials such as metals, often high laser power is required. This causes a potential problem to the use of laser techniques to produce conducting patterns on flexible and/or polymeric substrates as the high power laser could readily cut through the substrate while removing the metal layer. However, with careful adjustments of laser parameters from the calibration curve as shown in this manuscript, we found the use of CPs as a sacrificial layer to pattern metals using laser engraving technique.

In this manuscript, we report for the first time a micropatterning method for conducting layers on breathable substrate using laser engraving technique. CPs, metals on the sacrificial CP layer and graphene on non-conducting/porous/flexible substrates were successfully laser-etched. The calibration of the power and speed of the laser beam was performed and used to minimize the heat-affected zone (HAZ). OECTs were then fabricated using the laser engraving technique and were used in a gas sensor application.

EXPERIMENTAL

Materials

Substrate used was ePTFE (GORE-TEX®), and will be referred to as Gore-Tex throughout the manuscript, for all conducting materials. Conducting materials used were vapour phase polymerized (VPP) PEDOT, VPP thiophene, graphene (see deposition sections below) and thin gold layer (~50 nm) sputter-coated on VPP PEDOT.

Vapour Phase Polymerization of CPs

2,2′-Bithiophene (BTh) and 3,4-ethylenedioxythiophene (EDOT) were supplied by Sigma-Aldrich. Ferric *p*-toluenesulfonate (Fe(III)PTS) in 40% butanol was obtained from YACOO Chemical Reagent. All materials were used without further purification. For vapor phase polymerization,[13,32] Fe(III)PTS solution was spin-coated onto the desired substrate using a Laurell spin-coater at 1500 RPM for 30 sec. A closed chamber with monomer and the oxidant coated sample was placed in the oven at 70°C. The polymerization time was 1 hour for poly(-thiophene) and 30 min for PEDOT. Polymerized films were left to cool down to room temperature, rinsed carefully with ethanol, and kept in ethanol for about 12 hours. The films were rinsed with ethanol and left to dry overnight at room condition before use.

Graphene Deposition

Colloidal graphene was synthesized by chemical reduction of graphene oxide as reported by Li *et al.*[33] Colloidal graphene thickness after casting on Si wafer was measured using AFM to be 1 nm.[33] Maleic anhydride was plasma polymerized onto Gore-Tex substrate to induce desired surface functional groups and wettability. Graphene was deposited using Layer by Layer (LbL) method.[34] Polyallylamine hydrochloride (PAH, $M_w = 70{,}000$ g/mol) and polystyrenesulfonate, sodium salt (NaPSS $M_w = 70{,}000$ g/mol) were used as polyelectrolytes in 0.5*M* NaCl solutions with 0.9 mg/mL and 1 mg/mL concentration, respectively. Polyanionic and polycationic solution (with graphene) were deposited for 20 min, followed by DI water wash for 10 min. After three bilayer deposition the substrate was heat treated to 150°C for 120 min to achieve better conductivity.

Patterning Procedure

Pattern design was performed using AutoCAD software. A Versa Laser 3.50 laser engraver was used to pattern the material according to the designs. The laser used in the engraving process was a CO_2 laser with a wavelength of 10.6 μm and a nominal power of 40 W. Laser power and patterning speed was adjusted depending on conducting layer thickness and substrates used. Resolution can be adjusted using previously made calibration curves, where resolution is basically size of HAZ. After loading the desired pattern, manufacturing was started. More information regarding pattern preparation can be found in Supporting Information Figure S1. Patterning time is dependent on the speed, size of the area and pattern complexity. Patterning of 5 × 5 cm area normally takes a couple of minutes. Prepared sample can be washed in distilled water or ethanol to remove impurities produced during patterning process; however most of engraving machines have built-in exhaust system which efficiently removes dust produced during the process.

Laser Calibration

The depth of the lasered patterns was measured using Veeco Dektak 150 stylus profilometer and the HAZ size was estimated from microscopic images taken on a Nikon Eclipse ME600 microscope equipped with PixeLink PL-A662 CMOS camera.

Transistor Characterization

"Dog bone" transistor architecture was patterned on flexible Gore-Tex substrate. 0.1*M* sodium chloride (NaCl) was used as the electrolyte. The small PEDOT strip was used as a source-drain channel and big PEDOT strip as a gate electrode. Transistor characteristics were measured using a Keithley 2612A Sourcemeter and customized Labview software. I-V characteristics were performed by sweeping source-drain voltage and measuring corresponding current. Voltage was swept from 0 to −0.6V with voltage step of 0.1V. This procedure has been repeated for different gate electrode voltages, starting from 0V and going up to 0.7V with 0.1V voltage step. Time characteristics measurement was also carried out using a Keithley 2612A Sourcemeter, the drain-source voltage was kept at −0.5V, while a square voltage pulse for duration of 10 sec was applied to the gate, allowing 10 sec recovery periods. The gate voltage was stepped from 0.1 to 0.8V with 0.1V intervals. The experiments were performed under open-air condition.

Gas Sensing Set-Up and Procedures

As shown in Figure 5b, the gas sensing set-up consists of N_2 purging chamber (top), electrolyte/PEDOT electrode chamber (middle) and variable gas chamber (bottom). N_2 was purged through the electrolyte to get rid of any possible influence from oxygen. The bottom chamber for oxygen testing was purged with 0 (pure N_2), 21 (air) and 100% oxygen gas whereas for SO_2 testing it was purged with 0, 0.8, 4.1, and 8.1 % SO_2 gas produced from chemical reaction between sodium metabisulfite ($Na_2S_2O_5$) and HCl (see more detail in SI Figure S4) with N_2 as the carrier gas. To clean up the cell and recover PEDOT, N_2 was purged thoroughly for several minutes between each measurement. The other parameters for OECT

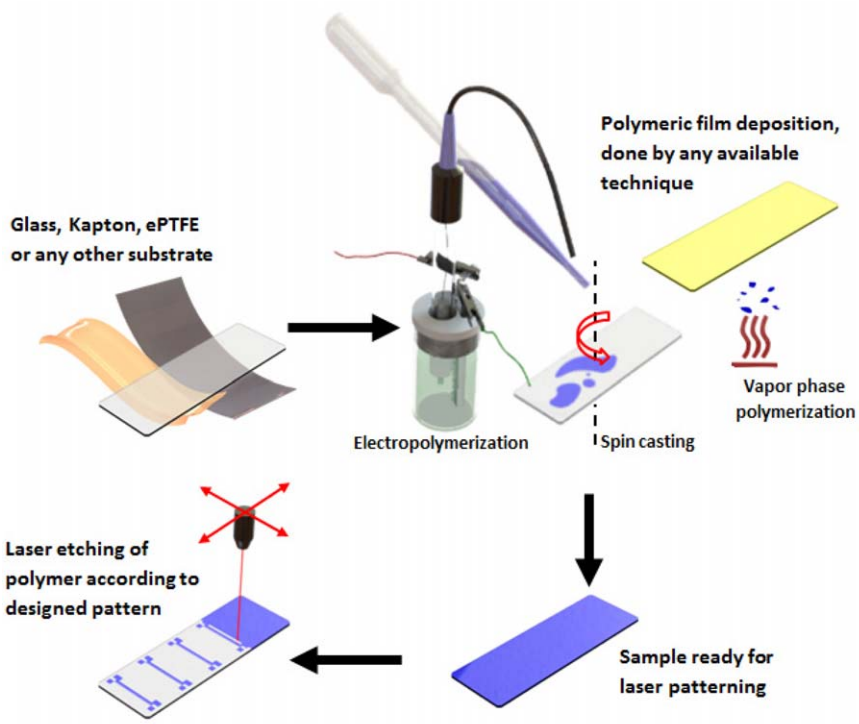

Figure 1. Schematics of patterning process for CPs on different substrates using laser engraving technology. [Color figure can be viewed in the online issue, which is available at wileyonlinelibrary.com.]

set-up were the same as described in "Transistor Characterization" section.

Electron Microscopy

SEM images were obtained using JEOL 7100F Field Emission Gun Scanning Electron Microscope at 5 kV. Experiments were performed on gold sputter-coated samples.

RESULTS AND DISCUSSION

The method described below uses a subtractive non-contact manufacturing technique, where material is removed in a controlled manner i.e. a polymer layer is exposed to a laser beam and is precisely removed following a given pattern. The steps involved in manufacturing of the desired pattern are shown in Figure 1. First, the surface of the substrate was coated with the desired polymer. Although a wide range of different substrate materials with different degree of flexibility including hard and relatively brittle materials like ceramics and glass, through to polymeric substrates such as Kapton, Mylar, PES and PVC, to membranes based on ePTFE can generally be used, only a breathable membrane based on ePTFE (Gore-Tex) is the focus of this report. Methods of deposition of the conductive layer can differ, depending on personal preferences or application needs. The three most commonly used techniques for deposition of CPs are chemical vapor deposition (including vapor phase polymerization), electro-polymerization or solution casting. All three techniques have been proven to be suitable for the described patterning method. The substrate with the deposited layer of CP was then exposed to the laser beam and removed following previously designed pattern. More information on pattern preparation can be found in Supporting Information Figures S1 and S2. Patterned samples can be rinsed with a solvent such as ethanol to remove dust and later dried, or can be used straight away. The resolution and speed of the laser patterning strongly depends on the quality of the laser equipment. The laser engraver used in this work is in the $10,000 range where the resolution as low as 30 μm can be achieved with a patterning speed approximately 10 cm^2/min. This is thus leaving scope for significant improvement in both resolution and speed with more advanced engraver equipment.

The described technique provides a fast and easy way for prototyping, giving complete flexibility regarding the substrate, conducting material as well as the pattern itself. Figure 2 shows "dog bone" transistor architecture manufactured from PEDOT on Gore-Tex using the described technique [Figure 2(a)], SEM image of PEDOT on Gore-Tex [Figure 2(b)] and its cross section [Figure 2(c)] with three distinguishable areas. The upper section of Figure 2(b) shows Gore-Tex substrate, while lower section is PEDOT coated Gore-Tex. The middle section is the transitional area (HAZ) between PEDOT coated Gore-Tex and Gore-Tex, which is basically burned and carbonized material from the decomposition of PEDOT. This transitional section is the result of heat convection in the material.

Figure 3 is an example of calibration parameters obtained for PEDOT layer on theGore-Tex substrate. Similar calibration for poly(thiophene) on Gore-Tex can be found in Supporting Information Figure S3.

Using the calibration parameters, laser etching of PEDOT on Gore-Tex membrane was performed and the results are shown

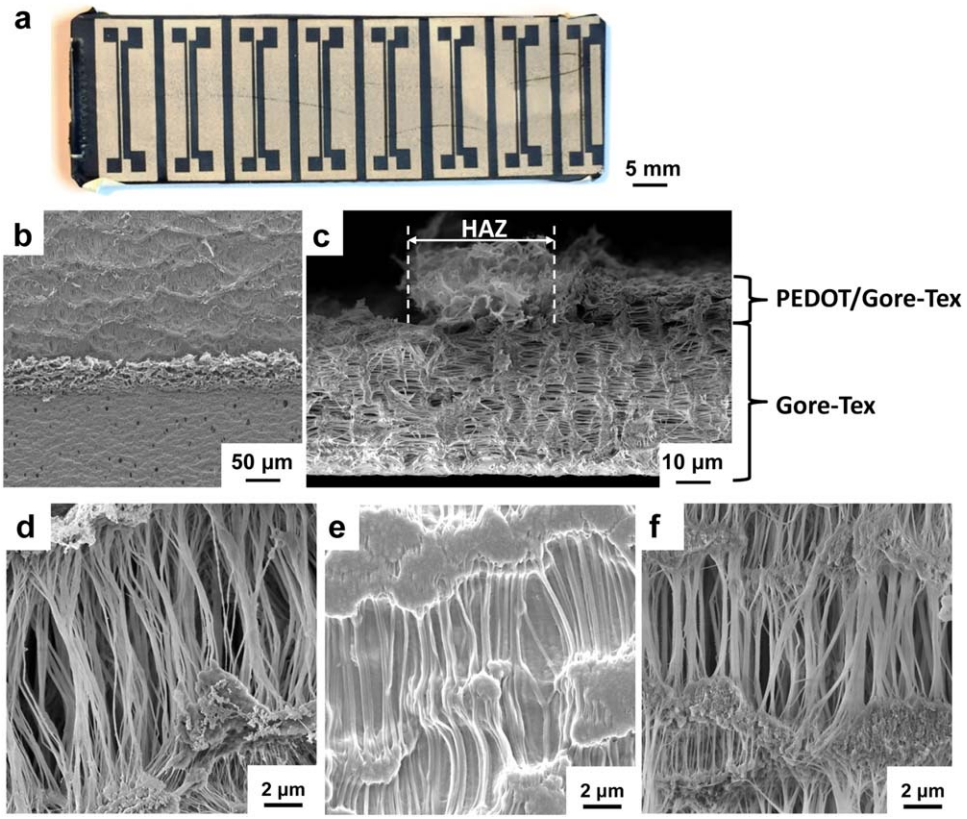

Figure 2. Images of PEDOT coated Gore-Tex and Gore-Tex: (a) Image of the "dog bone" PEDOT transistors patterned on Gore-Tex, (b) SEM image of the patterned transistor showing Gore-Tex (top), HAZ (middle) and PEDOT on Gore-Tex (bottom) layers, (c) Cross-sectional SEM image of the laser-etched PEDOT coated on Gore-Tex with visible HAZ, (d) bare, untreated Gore-Tex, (e) Gore-Tex membrane with deposited PEDOT, (f) Gore-Tex where PEDOT has been removed using laser engraving technique. [Color figure can be viewed in the online issue, which is available at wileyonlinelibrary.com.]

in Figure 2 as aforementioned. HAZ is not exposed directly to the laser beam, but it is affected (damaged) by the absorbed heat [Figure 3(a)]. The heat from the laser etching process and subsequent re-cooling causes this unwanted change in polymer-substrate interfaces as seen in Figure 2(c) that the Gore-Tex was deformed and the pores collapsed. The thermal diffusivity of both the substrate and patterning material play a large role in the HAZ size. However, due to bigger volume of substrate material compared to the volume of conducting layer, thermal diffusivity of the substrate material is considered more important. If thermal diffusivity is high, the material cooling rate is high, and the HAZ is relatively small. On the other hand, a low thermal diffusivity leads to slower cooling and a larger size of the heat-affected zone. The amount of heat introduced by the laser plays an important role in the process; high heat input is related to increase in HAZ size [Figure 3(c)]. The heat input (Q) is depending on the laser power as well as the speed of whereby the laser is moved and can be calculated using the following formula.[35,36]

$$Q = \left(\frac{P \times 60}{S \times 1000}\right) \times \eta \quad (1)$$

where Q is the heat input (kJ/mm), P is the laser power (W), S is the etching speed (mm/min.) and η is efficiency. The efficiency is dependent on the gas medium the laser beam travels through, distance between laser unit and the sample, scattering on the surface of the samples, laser wavelength relative to the absorption of the material being etched, working mode—pulsed or continuous, as well as few other parameters. The laser used in this study was a CO_2 laser with a wavelength of 943 cm^{-1}, which is overlapping with the absorption of the C—S vibration in PEDOT.[32] Normally, the efficiency factor for metal welding or metal cutting procedures is measurable and well established.[37] The efficiency value used was based on what is found and used for metallic materials as the materials used in the manuscript are also conducting materials with high heat dissipation similar to metals. Efficiency value used for the presented method is 0.95 for all materials reported in this paper.

With careful adjustment of the parameters such as laser power [Figure 3(b,c)] and engraving speed and mode [Figure 3(d)], laser etching process can give a highly concentrated, relatively uniform and limited amount of heat, resulting in a small HAZ. The data collection is done by varying laser power and the speed; and measuring corresponding pattern depth [Figure 3(b)] and HAZ [Figure 3(c)]. The gathered data is then plotted and the fitted and calibration curves can be used to find the right laser parameters for desired thickness of the conductive layer and desired quality/pattern resolution. It has to be noted that calibration curves are specific for conductive layer–substrate combination. Changing either substrate or conductor will require laser recalibration and subsequent curve fitting. This is due to change in heat dissipation between the two materials.

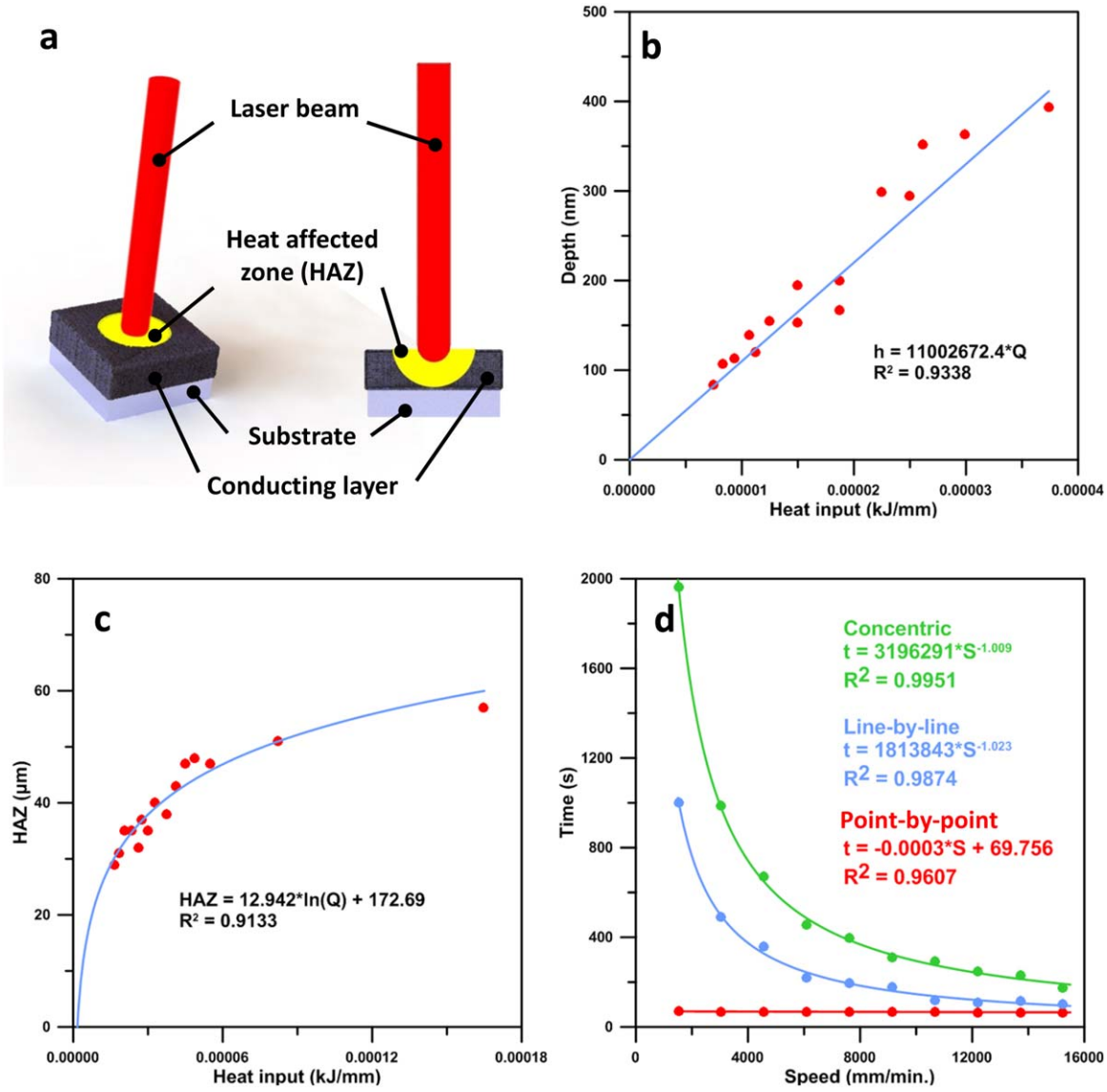

Figure 3. Calibration parameters for PEDOT layer on Gore-Tex substrate, (a) Schematic of PEDOT laser patterning with distinguished laser beam and HAZ, (b) Calibration of the laser power for different conducting layer thicknesses, (c) Size of the HAZ versus laser power. (d) Patterning time versus patterning speed for 25 cm^2, point-by-point method (bottom red trace), line-by-line (middle blue trace), concentric method (top green trace) (see more information on patterning preparation in Figure S1). [Color figure can be viewed in the online issue, which is available at wileyonlinelibrary.com.]

SEM cross section [Figure 2(c)] shows how precisely the patterned material can be removed from the sample without causing damage to the substrate material. This is very important when substrate material plays a functional role, like Gore-Tex in Figure 2 being a breathable porous membrane. The total thickness of the Gore-Tex membrane used is around 78 μm, while thickness of the PEDOT coated area is about 13 μm (calculated from the calibration curve [Figure 3(b)], the Q used was about 0.0012 kJ/mm to etch 13 μm) and the thickness of the Gore-Tex membrane after etching is about 64 μm. PEDOT has been removed without affecting the membrane structure and hence the breathing function of the membrane. SEM images of untreated Gore-Tex and Gore-Tex after laser etching are shown in Figure 2(d) and 2f confirming Gore-Tex structure and porosity are not changed by the laser, while PEDOT layer is completely removed. Image of PEDOT coated Gore-Tex [Figure 2(e)] is also provided as a reference.

Patterning of conducting layers on porous breathable substrate was further extended to patterning of metals and graphene. Creating patterns in gold, platinum and several other metals, can be a challenge due to their mechanical properties, roughness, and light scattering and light reflection on the surface. Fast heat dissipation and processability of the material can be additional issues. With carefully chosen laser parameters, we have shown that these issues can be overcome when laser patterning metals on breathable substrate. A thin layer of gold or platinum (~50 nm) was sputtered on top of a PEDOT sacrificial layer. When the laser beam hit the metal layer this heats up the underlying, highly thermally conducting PEDOT, which is then removed (sublimed) due to the heat as it cannot

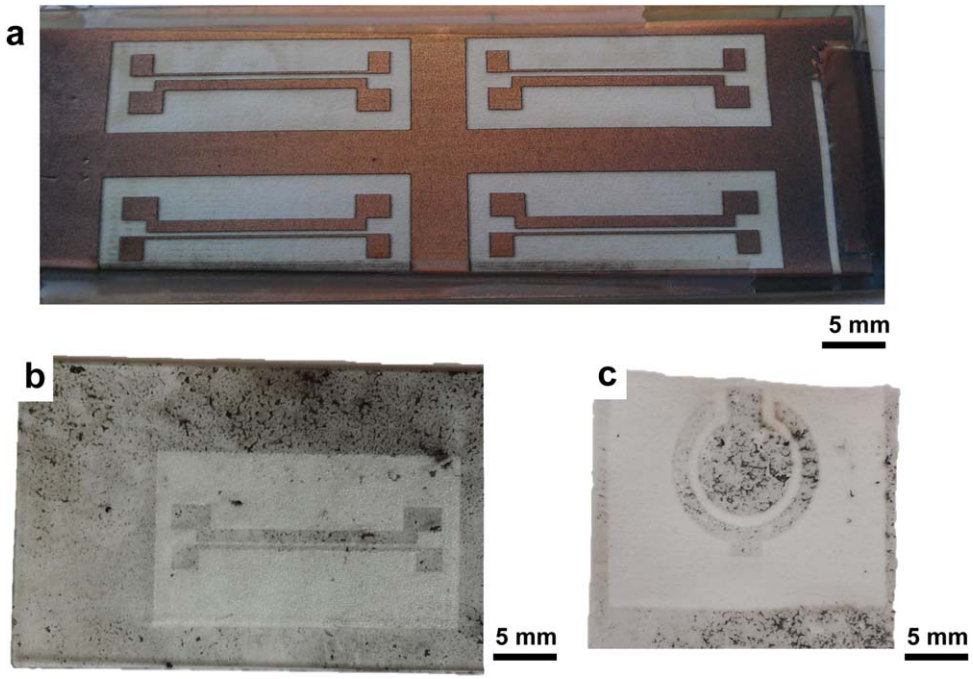

Figure 4. Various conducting materials patterned using the laser engraving technique (a) Gold "dog bone" transistor architecture patterned on flexible Gore-Tex substrate using PEDOT as sacrificial layer (b) Graphene "dog bone" transistor architecture on glass and (c) graphene capacitor patterned on Gore-Tex substrate. [Color figure can be viewed in the online issue, which is available at wileyonlinelibrary.com.]

transfer the heat fast enough to the membrane (low thermal conductivity) material.[30] The metal layer was removed together with sacrificial PEDOT and the desired shape of highly conductive circuits was formed as shown in Figure 4(a). This can find application where layers with high electrical conductivity are required.

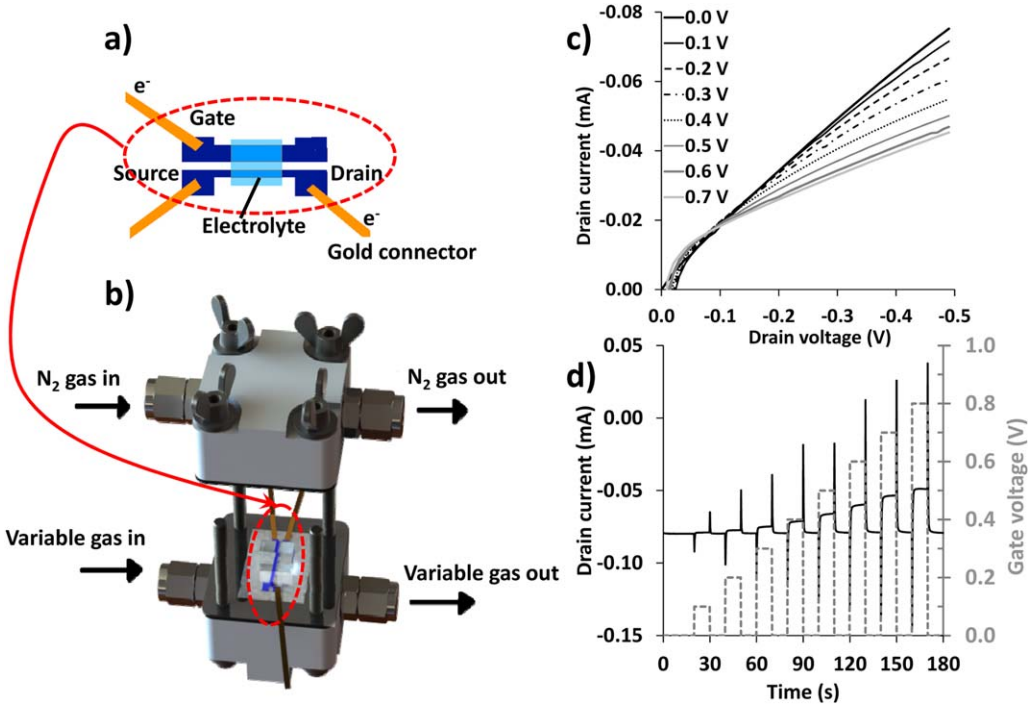

Figure 5. PEDOT OECT schematic and results. (a) schematic of OECT set-up and working principle, (b) semi-opened OECT/gas sensing cell set-up, (c) Transistor I-V output characteristics (operated in air) for gate voltage varying from 0 (top curve) to +0.7 V (bottom curve) with a step of 0.1 V, (d) Time characteristics (operated in air), where black line is a drain current and grey line is a gate voltage characteristics. [Color figure can be viewed in the online issue, which is available at wileyonlinelibrary.com.]

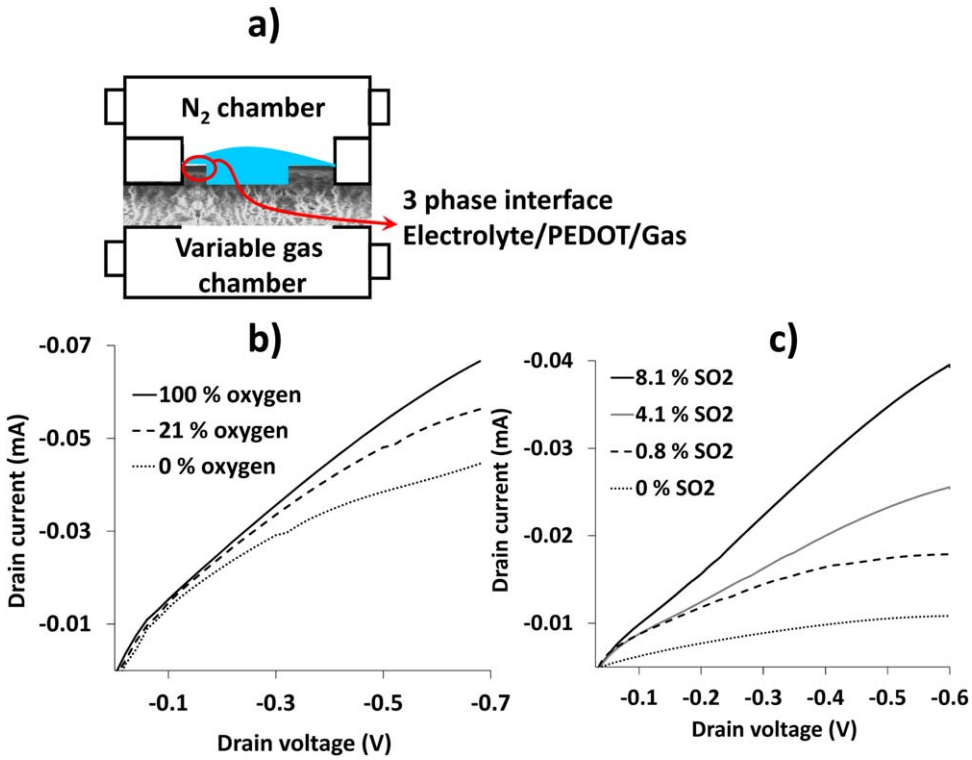

Figure 6. Gas sensing. (a) cross section of sealed gas sensing cell, (b) changes in drain current from drain potential sweep at various oxygen contents, (c) changes in drain current from drain potential sweep at various SO_2 contents. [Color figure can be viewed in the online issue, which is available at wileyonlinelibrary.com.]

The developed patterning procedure is also found to be useful for prototyping graphene circuits, where graphene is deposited via chemical reduction of graphene oxide[33] and later removed with the laser, forming desired circuit pattern [Figure 4(b,c)]. This is a novel graphene patterning technique. Previously developed graphene patterning method[38] uses reverse - additive approach where graphene oxide is reduced while forming patterns. Investigation on the use of metals or graphene conductive pattern on breathable substrate is underway and will be reported elsewhere.

PEDOT transistors (OECTs) on Gore-Tex, patterned using the laser engraving technique, were then characterized. Figure 5(a) depicts PEDOT OECT set-up and its brief working principle (for more detail on device set-up description and measuring procedure please see Experimental section). The channel [the thinner strip of the dog bone in Figure 5(a)] width was 0.2 mm and the channel length where it is exposed to the electrolyte was 5 mm. The whole length of the dog bone was 18 mm. The OECT and gas sensing set-up as the whole cell is shown in Figure 5(b). The transistor performance tests are shown in Figure 5(c) and 5d below. Both I-V characteristics and time characteristics of the laser-etched transistor are comparable in terms of electrical performance and signal amplification ability to similar devices reported elsewhere fabricated by photolithography[39,40] indicating that the laser patterning method is not influencing the transistor performance. Maximum transconductance value in neutral pH electrolyte was 63 μS (equals to 315 μS/mm normalized to the channel width, at the gate voltage of 0.3V for a 0.5V drain voltage) which is relatively high compared to the typical values obtained from PEDOT based OECTs.[41,42]

It is notable that the reduction of oxygen is occurring on the channel electrode. At less negative drain potentials (from ca. −0.15V and higher) the OECT is operating outside the potential range where oxygen reduction occurs and thus the drain current is not depending on the oxygen content before a sufficient negative drain potential is reached. Therefore, there was no observable difference in drain current at less negative drain voltage.

PEDOT OECTs were then used as gas sensors. A cross section of the sealed gas-sensing cell is shown in Figure 6(a) below. Gas flows through the Gore-Tex membrane from the back side of the PEDOT-coated Gore-Tex electrode and nitrogen was purged on the PEDOT side to maintain "zero" oxygen level on the electrolyte side. Here, the performance of the critical three phase interface [electrolyte/PEDOT/gas - red circle in Figure 6(a)] was tested in a configuration where the OECT is used as gas-sensor where a gas (oxygen or SO_2) is participating in a redox reaction on the PEDOT source/drain material and thereby contributes to the drain current. Various contents of oxygen or SO_2 gas were exposed to the Gore-Tex membrane side and the resulting drain current [Figure 6(b,c), respectively] measured at a fixed gate voltage. Preliminary gas sensing results indicated that the PEDOT coated Gore-Tex OECTs are working as gas sensors where the demonstrated sensing range of PEDOT OECT sensors was 0–100% for oxygen and 0.8–8.1% for SO_2. For oxygen

sensors, multiple devices from different polymerisation batches ($n = 3$) were tested and the deviation of the results are within the range of ±37% RSD. However, the SO_2 gas sensing has been performed based on a single device. This shows that the desired diffusion of gas through the membrane to the three phase interface was successful using the laser patterning technique i.e. not blocking the membrane structure.

The sensing mechanism is believed to be as follows. The gas sensing relies on PEDOT's ability to electrochemically reduce oxygen and oxidize SO_2 in the potential range where the OECT can operate. For the SO_2 sensor the oxidation reaction takes place on the gate electrode, where a positive potential is applied. This leads to an increased gate-current, which is being amplified by an increase in current of the channel electrode. The oxygen reduction is, in the reported configuration, occurring on the channel electrode where the presence of oxygen allows the PEDOT to remain in a relatively more oxidized (and thereby more conducting) state compare to the situation without presence of oxygen.[43]

As shown above, a procedure was developed for fabrication of OECTs on flexible and porous substrates for sensors. The gas can be purged directly into the cheap breathable OECT set-up for analysis rather than using expensive and high maintenance instruments such as gas chromatography or other spectroscopic methods. Potential applications include a much wider range of possibilities, for example, miniaturizing CP based electrodes for sensing applications. One example is to make a compact alcohol vapor sensor previously developed for bulk testing.[16]

The obtained three phase interface has been used in an OECT configuration in this report but the concept is surely not limited to this type of gas sensing device.

CONCLUSIONS

We have shown a fast and efficient way of manufacturing different CP patterns on a very porous and flexible substrate and demonstrated their use for OECT gas-sensing applications. Patterning that doesn't require expensive shadow masks and has flexibility of pattern adjustment in AutoCAD or other software, as demonstrated in this report, is a great advantage especially for rapid prototyping. This method has also proven to be efficient for patterning metal layers (gold, silver, platinum, etc.) where the CP serves as a sacrificial layer. Improving the resolution to industrial standards of around 10 μm is of great interest and the work to follow up and improve the technique is underway.

Notes: The authors declare no competing financial interest. Authors declare that the submitted work is their own and that copyright has not been breached in seeking its publication. The submitted work has not previously been published in full, and is not being considered for publication, elsewhere.

B.W-J. and B.K. initiated the study, designed experiments and established the patterning method. B.K. prepared samples, performed transistor and oxygen sensing measurements, and wrote the manuscript. S.S.N. prepared graphene samples, O.W-J. performed SEM. B.P. performed SO_2 gas sensing experiments. B.W-J. coordinated the project. The manuscript was written through contributions of all authors. All authors have given approval to the final version of the manuscript.

ACKNOWLEDGMENTS

B.W-J. and B.K. gratefully acknowledge the Australian Research Council for funding (DP110105461). Prof Douglas MacFarlane is acknowledged for valuable discussions. The authors acknowledge Monash University Centre for Electron Microscopy for providing electron microscopic facilities.

REFERENCES

1. Hwang, H. S.; Zakhidov, A. A.; Lee, J. K.; André, X.; Defranco, J. A.; Fong, H. H.; Holmes, A. B.; Malliaras, G. G.; Ober, C. K. *J. Mater. Chem.* **2008**, *18*, 3087.
2. Taylor, P. G.; Lee, J. K.; Zakhidov, A. A.; Chatzichristidi, M.; Fong, H. H.; DeFranco, J. A.; Malliaras, G. G.; Ober, C. K. *Adv. Mater. (Weinheim, Ger.)* **2009**, *21*, 2314.
3. Zakhidov, A. A.; Fong, H. H.; Defranco, J. A.; Lee, J. K.; Taylor, P. G.; Ober, C. K.; Malliaras, G. G.; He, M.; Kane, M. G. *Appl. Phys. Lett.* **2011**, *99*, 183308.
4. Ito, Y.; Onodera, Y.; Tanabe, R.; Ichihara, M.; Kamada, H. *Proc. SPIE-Int. Soc. Opt. Eng.* **2007**, *6458*, 64580C.
5. Lasagni, A. F.; Hendricks, J. L.; Shaw, C. M.; Yuan, D.; Martin, D. C.; Das, S. *Appl. Surf. Sci.* **2009**, *255*, 9186.
6. Dobroiu, S.; Delft, F. C. M. J. M. V.; Thiel, E. V.; Hanson, K. L.; Nicolau, D. V. *Microelectron. Eng.* **2010**, *87*, 1190.
7. Liang, J.; Chen, Y.; Xu, Y.; Liu, Z.; Zhang, L.; Zhao, X.; Zhang, X.; Tian, J.; Huang, Y.; Ma, Y.; Li, F. *ACS Appl. Mater. Interfaces* **2010**, *2*, 3310.
8. Petsch, T.; Haenel, J.; Clair, M.; Keiper, B.; Scholz, C. *Proc. SPIE-Int. Soc. Opt. Eng.* **2011**, *7921*, 79210U.
9. Xiao, S.; Abreu Fernandes, S.; Esen, C.; Ostendorf, A. *J. Laser Micro/Nanoeng.* **2011**, *6*, 249.
10. Toossi, A.; Daneshmand, M.; Sameoto, D. *J. Micromech. Microeng.* **2013**, *23*, 047001.
11. Rajput, D.; Costa, L.; Lansford, K.; Terekhov, A.; Hofmeister, W. *ACS Appl. Mater. Interfaces* **2013**, *5*, 1.
12. Yang, C. C.; Hsiao, W. T.; Chung, C. K.; Tsai, H. Y.; Yeh, J. L. A.; Huang, K. C. *Appl. Phys. A: Mater. Sci. Process.* **2014**, 1.
13. Winther-Jensen, B.; Winther-Jensen, O.; Forsyth, M.; MacFarlane, D. R. *Science* **2008**, *321*, 671.
14. Winther-Jensen, B.; MacFarlane, D. R. *Energy Environ. Sci.* **2011**, *4*, 2790.
15. Winther-Jensen, O.; Chatjaroenporn, K.; Winther-Jensen, B.; MacFarlane, D. R. *Int. J. Hydrogen Energy* **2012**, *37*, 8185.
16. Winther-Jensen, O.; Kerr, R.; Winther-Jensen, B. *Biosens. Bioelectron.* **2014**, *52*, 143.
17. Mabeck, J. T.; Malliaras, G. G. *Anal. Bioanal. Chem.* **2006**, *384*, 343.
18. Owens, R. M.; Malliaras, G. G. *MRS Bull.* **2010**, *35*, 449.
19. Facchetti, A. *Nat. Mater.* **2013**, *12*, 598.

20. Noh, Y.-Y.; Zhao, N.; Caironi, M.; Sirringhaus, H. *Nat. Nano.* **2007**, *2*, 784.
21. Sandström, A.; Dam, H. F.; Krebs, F. C.; Edman, L. *Nat. Commun.* **2012**, *3*, 1002.
22. Miura, H.; Fukuyama, Y.; Sunda, T.; Lin, B.; Zhou, J.; Takizawa, J.; Ohmori, A.; Kimura, M. *Adv. Eng. Mater.* **2014**, 550.
23. Tria, S. A.; Jimison, L. H.; Hama, A.; Bongo, M.; Owens, R. M. Biochim. Biophys. Acta, *Gen. Subj.* **2012**, *1830*, 4381.
24. Bongo, M.; Winther-Jensen, O.; Himmelberger, S.; Strakosas, X.; Ramuz, M.; Hama, A.; Stavrinidou, E.; Malliaras, G. G.; Salleo, A.; Winther-Jensen, B.; Owens, R. M. *J. Mater. Chem. B* **2013**, *1*, 3860.
25. Jang, J.; Chang, M.; Yoon, H. *Adv. Mater. (Weinheim, Ger.)* **2005**, *17*, 1616.
26. Winther-Jensen, B.; Krebs, F. C. *Sol. Energy Mater. Sol. Cells* **2006**, *90*, 123.
27. Winther-Jensen, B.; West, K. *React. Funct. Polym.* **2006**, *66*, 479.
28. Goto, H.; Yoneyama, H.; Togashi, F.; Ohta, R.; Tsujimoto, A.; Kita, E.; Ohshima, K.-I.; Daniel, R. *J. Chem. Educ.* **2008**, *85*, 1067.
29. Bhattacharyya, D.; Howden, R. M.; Borrelli, D. C.; Gleason, K. K. *J. Polym. Sci., Part B: Polym. Phys.* **2012**, *50*, 1329.
30. Brooke, R.; Evans, D.; Dienel, M.; Hojati-Talemi, P.; Murphy, P.; Fabretto, M. *J. Mater. Chem. C* **2013**, *1*, 3353.
31. Kubis, P.; Li, N.; Stubhan, T.; Machui, F.; Matt, G. J.; Voigt, M. M.; Brabec, C. *J. Prog. Photovoltaics Res. Appl.* **2015**, *23*, 238.
32. Winther-Jensen, B.; West, K. *Macromolecules* **2004**, *37*, 4538.
33. Li, D.; Muller, M. B.; Gilje, S.; Kaner, R. B.; Wallace, G. G. *Nat. Nano.* **2008**, *3*, 101.
34. Rani, A.; Song, J.-M.; Jung Lee, M.; Lee, J.-S. *Appl. Phys. Lett.* **2012**, *101*, 233308.
35. Steen, W. M.; Mazumder, J. Laser Material Processing, 4th ed., **2010**.
36. Shin, H. M.; Choi, H. W. *Int. J. Adv. Manuf. Tech.,* DOI: 10.1007/s00170-014-6241-5.
37. Quintino, L.; Liskevich, O.; Vilarinho, L.; Scotti, A. *Int. J. Adv. Manuf. Tech.* **2013**, *68*, 2833.
38. Gao, W.; Singh, N.; Song, L.; Liu, Z.; Reddy, A. L. M.; Ci, L.; Vajtai, R.; Zhang, Q.; Wei, B.; Ajayan, P. M. *Nat. Nano.* **2011**, *6*, 496.
39. Shim, N. Y.; Bernards, D.; Macaya, D.; DeFranco, J.; Nikolou, M.; Owens, R.; Malliaras, G. *Sensors* **2009**, *9*, 9896.
40. Yaghmazadeh, O.; Cicoira, F.; Bernards, D. A.; Yang, S. Y.; Bonnassieux, Y.; Malliaras, G. G. *J. Polym. Sci., Part B: Polym. Phys.* **2011**, *49*, 34.
41. Jimison, L. H.; Hama, A.; Strakosas, X.; Armel, V.; Khodagholy, D.; Ismailova, E.; Malliaras, G. G.; Winther-Jensen, B.; Owens, R. M. *J. Mater. Chem.* **2012**, *22*, 19498.
42. Bernards, D. A.; Malliaras, G. G. *Adv. Funct. Mater.* **2007**, *17*, 3538.
43. Kerr, R.; Pozo-Gonzalo, C.; Forsyth, M.; Winther-Jensen, B. *Electrochim. Acta* **2015**, *154*, 142.